Application of HDMI® Cables as an MRI Compatible Single Cable Solution for Readout and Power Supply of SiPM Based PET Detectors

Andrew L. Goertzen, *Member, IEEE*, Jonathan D. Thiessen, Xuezhu Zhang, *Member, IEEE*, Chen-Yi Liu, Eric Berg, Daryl Bishop, Piotr Kozlowski, Fabrice Retière, Vesna Sossi, Greg Stortz and Christopher J. Thompson, *Senior Member, IEEE*

Abstract— All PET detectors require cabling to supply power and transmit data, whether in analog or digital form. In this work we examine using High-Definition Multimedia Interface (HDMI®) cables as a single cable solution to both supply power and transmit analog signals for a SiPM based PET detector that will be used in a hybrid PET/MRI imaging system. HDMI cables are designed for digital audio/video transmission, with each cable having four pairs of shielded 100 ohm differential signal lines, each rated for 3.4 Gbit/s, along with 7 additional signal lines and a braided shield around the entire cable. While designed as a digital signal cable, the lines are rated for 40V DC and 0.5A current. To test using HDMI® cables for application in PET, a silicon photomultiplier (SiPM) PET detector module with a single HDMI® Type C ('mini) receptacle was built using a SensL SPMArray4 coupled to a dual-layer offset LYSO crystal array 1.67 mm crystal pitch. The 16 detector outputs were multiplexed to four signals using a simple resistor charge division network and driven using Analog Devices AD8132 op-amps. Detector bias of 30.2V and +/- 5V power for the op-amps was supplied through a 25' length HDMI® cable connected through a custom receiver card. The signals were processed using NIM electronics and digitized with a PC based analog to digital converter (ADC) card. The PET detector had an average energy resolution of 14.3% full-width at half-maximum (FWHM) and an average timing resolution of 2.50 ns. The performance of the PET detector was unaffected when operated inside a 7T MRI system. The MR images showed degradation in signal to noise ratio (SNR) of between 7 and 23%, which is believe to be due to coupling between the RF coil and the PET detector shielding. The results of this work suggest that HDMI® cables with the Type C connector are a viable, cost effective and robust single cable solution for both analog signal and power/bias transmission for an MRI compatible PET insert system.

Index Terms— PET, silicon photomultiplier, small animal PET, hybrid PET/MRI, scintillation detector cabling

I. INTRODUCTION

PET detectors, regardless of their design, require some form of power supply and data transmission lines in order to function. In a research and development environment, there are not practical limitations on the space required for power and signal connections so it is common to use 50Ω coaxial cable for each signal line and individual connectors for detector bias and power supplies. When multiple detectors are being used, either in a complete PET system or in a multi-detector benchtop test situation, the use of individual cables for each signal and power line can become prohibitive both in terms of cost and space required for the cables and their connectors. For these reasons it is desirable to have a single cable assembly that includes multiple lines and uses a robust connector.

In this work we investigate using standard High-Definition Multimedia Interface (HDMI®) cables as a single cable for both reading out and supplying power to PET detectors based on silicon photomultipliers (SiPMs). This cabling solution will ultimately be used in a MR compatible PET insert system under development in our group [1, 2]. HDMI cables and connectors have the advantage of being consumer devices and are thus readily available and low cost. They are also mechanically robust and are designed to survive a large number of mating/unmating cycles.

A.L. Goertzen is with the Departments of Radiology and Physics & Astronomy, University of Manitoba, Winnipeg, Manitoba, Canada. Phone: +1 (204) 975-7771, e-mail: Andrew.Goertzen@med.umanitoba.ca.

J.D. Thiessen and X. Zhang are with the Department of Radiology, University of Manitoba, Winnipeg, Manitoba, Canada.

C.-Y. Liu is with the Department of Physics & Astronomy, University of Manitoba, Winnipeg, Manitoba, Canada.

E. Berg was with the Department of Physics & Astronomy, University of Manitoba, Winnipeg, Manitoba, Canada. He is now with the Department of Biomedical Engineering, University of California, Davis, Davis, California, USA.

D. Bishop and F. Retière are with the Detector Development Group, TRIUMF, Vancouver, British Columbia, Canada.

P. Kozlowski is with the Department of Radiology, University of British Columbia, Vancouver, British Columbia, Canada.

V. Sossi and G. Stortz are with the Department of Physics & Astronomy, University of British Columbia, Vancouver, British Columbia, Canada.

C.J. Thompson is an Emeritus Professor of the Montreal Neurological Institute, McGill University, Montréal, Québec, Canada.
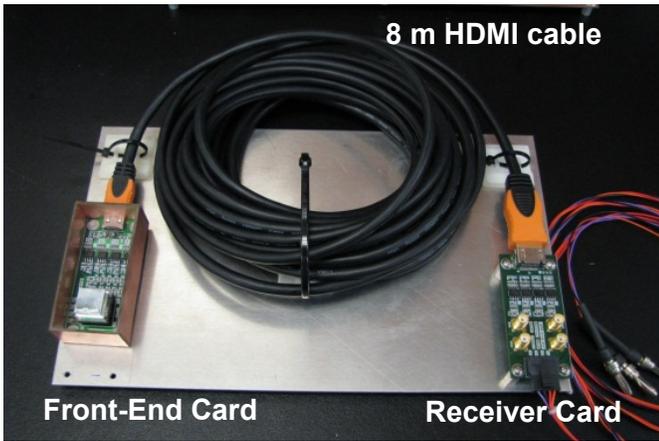
Fig. 1. Photo of the PET detector module connected by 8 m HDMI® cable to the receiver card that supplies power and has SMA outputs for interfacing detector signals to NIM electronics.

II. MATERIALS AND METHODS

A. HDMI® Cable Standard

The HDMI® interface is a 19 pin connection with multiple connector types including Type A (standard), Type C (mini) and Type D (micro) [3]. Of the 19 pins, 12 pins are dedicated to four shielded twisted pair 100Ω differential lines (one line each for data+, data- and shield) that normally are operated as the digital signals TMDS Data0, TMDS Data1, TMDS Data 2 and clock. The remaining 7 pins are normally dedicated to serial clock and data lines, +5V power, ground and hot plug detect. The cable is also shielded with a braid. While designed as a digital cable, the HDMI® cable has favourable characteristics for analog use. For example, the Molex model 687670022 cable (Type A to Type A, 5 m length) and Molex Type A receptacle 47151-0001 have an attenuation of less than 8 dB at 825 MHz, are rated to 40 V DC and 0.5 A of DC current and have an insulation resistance between adjacent pins of 150 V DC.

B. Detector and Detector Electronics Design

A PET detector, shown in Fig. 1, was constructed using a SensL SPMArray4 SiPM detector (SensL Inc., Cork, Ireland) coupled to a dual layer LYSO:Ce scintillator array that uses a half-crystal offset in the X and Y direction to decode layer information [1]. The array used in this work was comprised of a 7×7 crystal array bottom layer with thickness of 6 mm and crystal pitch of 1.67 mm and a 6×6 element top layer with thickness 4 mm and crystal pitch 1.67 mm. All crystal surfaces were polished and a bonded enhanced specular reflector (ESR) was used as the reflector between crystals. This crystal array was purchased from Proteus Inc. (Chagrin Falls, OH). The 16 outputs of the SiPM array are multiplexed through a resistor based multiplexing network [4] to reduce the number of outputs to 4. The outputs of the multiplexing network are input to four Analog Devices AD8132 differential output op-amps, whose outputs are driven through 49.9 Ω into the HDMI® cable twisted pair signal lines (i.e. pins 1-12) through an HDMI® mini (Type C) connector. The spare lines of HDMI® cable are used to supply detector bias (30.2V), +/- 5V and ground. There are two spare lines to allow future inclusion of
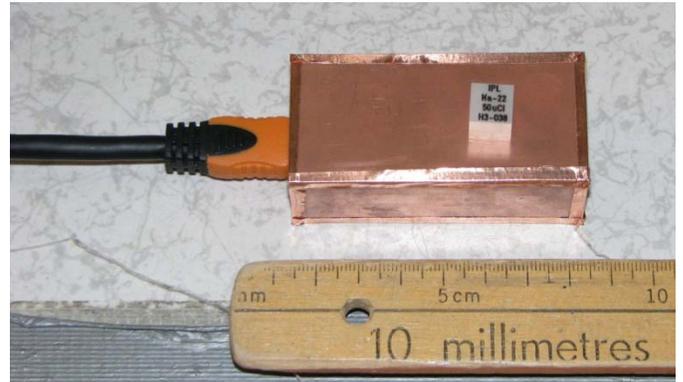

Fig. 2. Photo of sealed PET detector module with ²²Na source and HDMI® mini (Type C) cable connected.
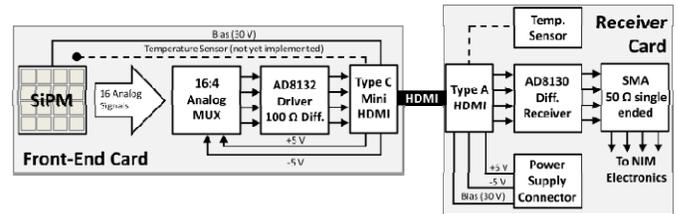

Fig. 3. Schematic diagram showing components on the front-end and receiver cards of the detector.

temperature monitoring. The entire front-end detector card is enclosed in a housing made of double sided copper clad printed circuit board (1 oz., FR4) and sealed at the seams with copper tape.

A receiver card with an HDMI® Type A connector was constructed to interface the HDMI® cable to standard power and signal lines. Analog Devices AD8130 differential receiver op-amps were used to convert the 100 Ω differential signals to 50 Ω single ended outputs for interfacing to standard NIM electronics via SMA connecter. The receiver card had power inputs for +/- 6V and detector bias (30.2V) and had onboard power regulators for the low voltage power. Fig. 3 shows a schematic of the front-end and receiver cards. In this work a 25' (7.62 m) long HDMI® cable was used. The cable, from BrightLink Cables (www.brightlinkcables.com) was HDMI® v1.4, Type A to Type C, 30 AWG cable with 24k gold plated connectors.
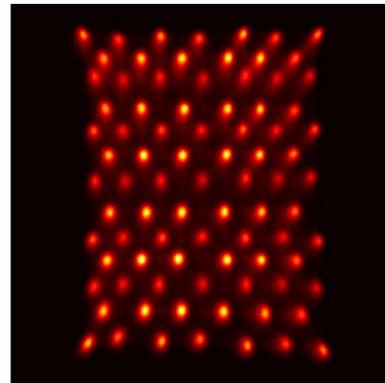

Fig. 4. Flood histogram of dual-layer detector acquired with 8 m long HDMI® cable. The dual-layer offset crystal design leads to interleaved locations of the upper and lower layer crystals, reducing layer identification to a simple problem of identifying a crystal in the flood histogram image.
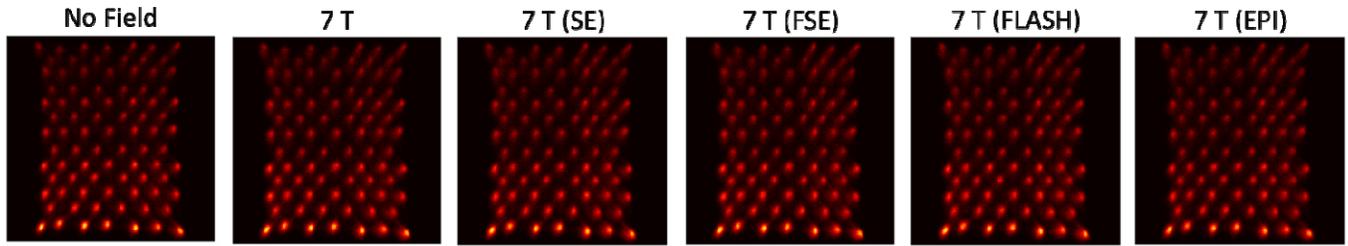
3185

Fig. 5. Flood histogram images acquired for the PET detector outside the MR (No Field), inside the MR with no MR sequence running (7 T) and with various MR pulse sequences running (SE, FSE, FLASH and EPI). The flood images show a gradient from top to bottom due to the placement of the [22]Na source at the end of the PET detector module. There were no noticeable changes in the flood histograms with applied MR sequences.

The analog outputs of the receiver card were processed using standard NIM electronics and digitized with a PC based ADC card as we have previously described [5]. The data were acquired using a custom LabWindows/CVI interface (National Instruments, Austin, TX) and data were processed using custom Matlab software and scripts (Mathworks, Natick, MA).

C. Performance Evaluation of Stand-Alone PET Detector Module

The detector was flood irradiated with a [68]Ge line source and the data used to create a flood histogram image. The flood image was segmented into individual crystal regions allowing energy spectra to be created on a per-crystal basis. The photopeak of the energy spectra were fit to a Gaussian curve to allow calculation of the full-width at half-maximum (FWHM) energy resolution for each crystal. The timing performance of the detector was evaluated by putting the detector in coincidence with a Scanwell Systems timing probe [6] (Scanwell Systems, Montréal, Québec), which consists of a plastic scintillator with embedded [22]Na source coupled to a fast PMT. The timing probe was used to start an Ortec 567 time to amplitude converter and single channel analyzer (TAC/SCA) and the detector providing the stop signal.

D. MRI Compatibility of Detector Module and Cable

The detector module was placed inside a Bruker 7T MRI system above a quadrature volume RF coil (25 mm ID, 30 mm axial extent). An H_2O, 1 g/l $CuSO_4 \cdot 5H_2O$ and 3.6 g/l NaCl phantom was placed inside the coil and used as the MR imaging phantom. B_0 and B_1 field maps were acquired together with image sequences using spin echo (SE), fast spin echo (FSE), fast low-angle shot (FLASH) gradient echo and echo planar imaging (EPI). The MRI setup and sequences were repeated with four different detector module setups: 1) no detector; 2) with the detector placed directly above the RF coil; 3) with the HDMI® cable attached to the detector but not powered up; and 4) during acquisition of PET detector flood histogram data. For flood image data a [22]Na source was attached to the RF coil immediately in front of the detector module. This placement of the source was such that the detector was irradiated from the end of the detector rather than with the source centered above the face of the detector. The PET detector performance was evaluated for flood histogram image quality and for energy resolution in these measurements. It was not possible to perform timing resolution measurements due to the incompatibility of the timing probe with the magnetic field.

III. RESULTS

A. Performance of Stand-Alone PET Detector Module

Fig. 4 shows the flood histogram image obtained from the detector module. The flood image showed no physical distortions, with all crystals being well resolved. The energy resolution, averaged over all crystals in a layer, was 14.4% ± 1.1% for the bottom layer and 14.1% ± 0.9% for the top layer. The timing resolution was 2.50 ns ± 0.15 ns for the bottom layer and 2.51 ns ± 0.14 ns for the top layer. Similar energy and timing results were obtained for a 6' length HDMI® cable (results not shown), suggesting that the long cable length does not degrade detector performance. The timing was largely limited by the slow intrinsic rise time of the SPMArray4 (~40 ns) for which we measured a FWHM timing resolution of 1.6 ns when reading out only a single pixel of the SPMArray4 with a dedicated AD8132 amplifier.

B. MRI Compatibility of PET Detector Module and Cable

Fig. 5 shows the PET detector flood histogram images acquired outside the MR, inside the MR and inside the MR with various MR sequences running during PET data acquisition. Table 1 gives the energy resolution for each crystal layer for each of the flood image datasets. The PET detector functioned well in the MRI system, showing no change in flood image appearance or energy resolution for any of the MRI sequences tested. A change was observed in the photopeak amplitude when the PET detector was placed inside the MR system, with the 511 keV photopeak at 4.3 ± 0.2V outside the magnet compared with 4.6 ± 0.3V inside the magnet. It is assumed that this difference is due to a decrease in the detector temperature, which was not monitored or corrected for in this work.

Fig. 6 shows the B_0 map images in the MR imaging phantom volume for the case of no detector present and the detector operating. As seen in Fig. 7, there was a slight shift

TABLE I
ENERGY RESOLUTION OF PET DETECTOR FOR DIFFERENT MRI SEQUENCES

	Bottom Layer	Top Layer
Outside MR	14.3 ± 1.2%	14.7 ± 1.4%
7T (No sequence)	14.3 ± 1.1%	14.8 ± 1.2%
7T (SE)	14.3 ± 1.2%	14.7 ± 1.2%
7T (FSE)	14.3 ± 1.1%	14.8 ± 1.1%
7T (FLASH)	14.3 ± 1.0%	14.7 ± 1.2%
7T (EPI)	14.3 ± 1.1%	14.8 ± 1.3%
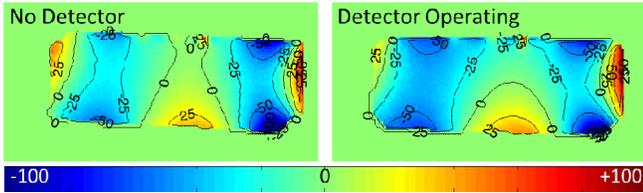
Fig. 6. B_0 maps showing deviation from Larmor frequency (in Hz) in the imaging phantom volume.

Fig. 8. B_1 map showing flip angle after an $\alpha=90°$ RF pulse in the imaging phantom volume.
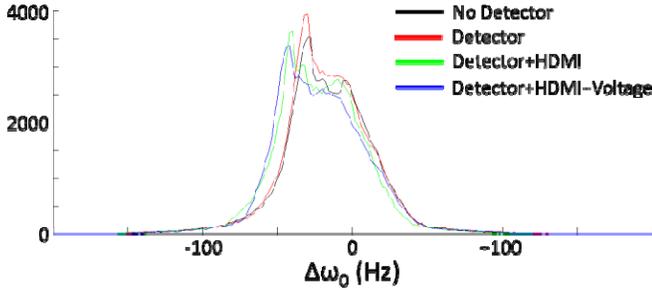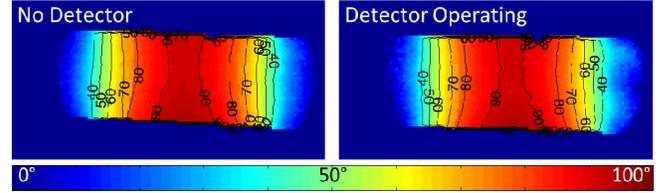

Fig. 7. Histogram of shift in Larmor frequency values in B_0 maps for different detector connection and operating cases. Attaching the HDMI® cable to the detector led to a slight downward shift in the Larmor frequency.

Fig. 9. Histograms of $|\Delta\alpha|$ values in phantom volume for the B_1 map images of Fig. 8.

downwards in the Larmor frequency caused by connecting the HDMI® cable to the PET detector module. Figs. 8 and 9 show a similar map and histogram for the B_1 uniformity. There was no significant impact on B_1 homogeneity caused by operating the PET detector inside the MR system.

Table II gives the signal to noise ratio (SNR) for the MR images for the four MR sequences evaluated for cases of no detector, detector only, detector plus cable and operating detector. For the operating detector there was a 7 to 23% decrease in the SNR of the MR image. It is currently believed that decrease in SNR is due to coupling between the RF coil and the shielding of the PET detector module and is not due to the HDMI® cable or receptacle. There was no significant change in the MR image homogeneity, as shown in Table III.

TABLE II
MRI SIGNAL TO NOISE RATIO FOR VARIOUS CASES OF MRI IMAGE SEQUENCE AND PET DETECTOR OPERATING CONDITION.

	No Detector	Detector Only	Detector + Cable	Detector Operating
SE	180 ± 5[a]	178 ± 6 (-1%)[b]	172 ± 6 (-4%)	146 ± 9 (-19%)
FSE	192 ± 12	180 ± 11 (-6%)	182 ± 14 (-5%)	176 ± 11 (-8%)
FLASH	81 ± 6	77 ± 6 (-5%)	76 ± 7 (-6%)	62 ± 8 (-23%)
EPI	NR*	530 ± 50	520 ± 50 (-1%)	490 ± 60 (-7%)

[a]Mean ± standard deviations calculated from 5 middle slices and 5 repetitions of each sequence.
[b](Percent change) calculated relative to first reported value in each row.
*Values not reported (NR) for first EPI sequence due to a different field of view.

TABLE III
MRI IMAGE HOMOGENEITY FOR VARIOUS CASES OF MRI IMAGE SEQUENCE AND PET DETECTOR OPERATING CONDITION.

	No Detector	Detector Only	Detector + Cable	Detector Operating
SE	95.1±0.4	94.5±0.6 (-0.6%)	94.3±0.9 (-0.8%)	94.2±0.8 (-0.9%)
FSE	89±3	88±3 (-0.7%)	89±3 (+0.8%)	89±2 (+0.6%)
FLASH	90±1	90±1 (+0.3%)	90±1 (+0.4%)	90±1 (-0.2%)
EPI	NR	95±1	96±2 (+0.8%)	96±1 (+0.7%)

IV. SUMMARY AND CONCLUSIONS

In this work an HDMI® cable with the 'mini' (Type C) connector was successfully used as a single cable connection for supplying bias, low voltage power and transmitting analog signals for a SiPM based PET detector operating inside a 7T MRI system. The PET detector showed no degradation in performance when operating simultaneously with MR image acquisition sequences however there was degradation in MRI SNR of between 7 and 23%. This degradation is believed to be due to coupling between the RF coil and the shielding of the PET detector module. Once this issue is addressed we believe there will be an improvement in the SNR measurements. The cables used in this work were 25' in length, similar to what would be used for a complete MR compatible PET insert system.

One limitation of using HDMI® cables as a single cable connection for reading out PET detector is that one is presently limited to SiPM detectors that use a bias voltage of less than 40V due to the 40V limit of the cable and the connector receptacles. For SiPM detectors, such as those from Hamamatsu, that use a bias voltage of ~70V one would have to use a second independent cable for supplying bias.

The results of this work suggest that HDMI® cables with the Type C connector are a viable single cable solution for both analog signal and power/bias transmission for an MRI compatible PET insert system. This simple cabling solution for our MRI compatible PET insert will facilitate system setup and insertion/removal from the MRI system. This will also facilitate system servicing and module replacement in the complete system.

REFERENCES

[1]   C. J. Thompson, A. L. Goertzen, E. J. Berg *et al.*, "Evaluation of High Density Pixellated Crystal Blocks With SiPM Readout as Candidates for PET/MR Detectors in a Small Animal PET Insert," *IEEE Transactions on Nuclear Science,* vol. 59, no. 5, pp. 1791-1797, 2012.

[2]   C. J. Thompson, G. Stortz, A. L. Goertzen *et al.*, "Comparison of Single and Dual Layer Detector Blocks for Pre-clinical MRI-PET," *Nucl Instrum Meth A*, In press, DOI:10.1016/j.nima.2012.07.062.

[3]   HDMI Licensing, LLC. 16 November 2012; www.hdmi.org.

[4]   A. L. Goertzen, M. M. McClarty, C. J. Thompson *et al.*, "Evaluation of a resistor network charge division multiplexing circuit for a 16 pixel SiPM array," in 2011 IEEE Nuclear Science Symposium and Medical Imaging Conference, Valencia, Spain, 2011.

[5]   B. McIntosh, D. B. Stout, and A. L. Goertzen, "Validation of a GATE Model of 176Lu Intrinsic Radioactivity in LSO PET Systems," *IEEE Transactions on Nuclear Science,* vol. 58, no. 3, pp. 682-686, 2011.

[6]   J. Hancock, and C. J. Thompson, "Evaluation of an instrument to improve PET timing alignment," *Nuclear Instruments and Methods in Physics Research Section A: Accelerators, Spectrometers, Detectors and Associated Equipment,* vol. 620, no. 2-3, pp. 343-350, 2010.